



Supplement of

On the drivers of droplet variability in alpine mixed-phase clouds

Paraskevi Georgakaki et al.

Correspondence to: Athanasios Nenes (athanasios.nenes@epfl.ch)

The copyright of individual parts of the supplement might differ from the article licence.

Supplemental Information

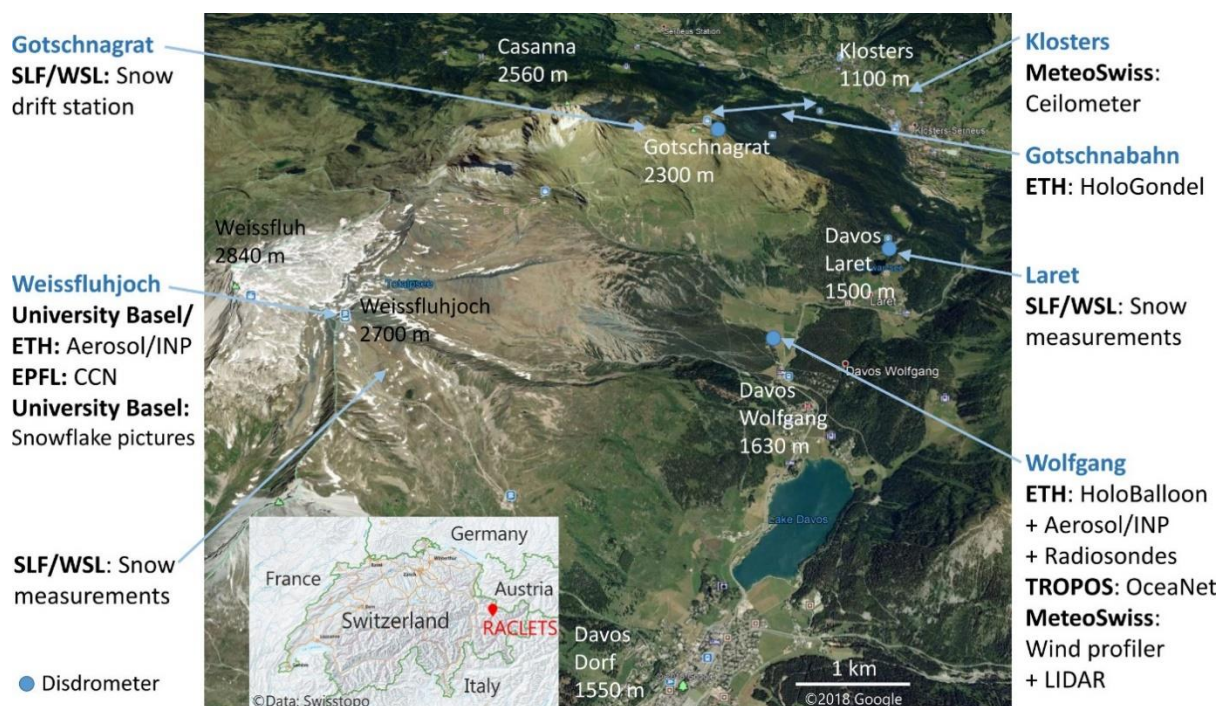


Figure S1. Location of the main measurement sites of the RACLETS 2019 campaign. The main measurement sites considered in this study are Davos Wolfgang (otherwise known as Wolfgang-Pass, WOP; 1630 m a.s.l., 46°50'08.076"N 9°51'12.939"E) and the mountain-top station of Weissfluhjoch (WFJ; 2700 m a.s.l., 46°49'58.670"N 9°48'23.309"E).

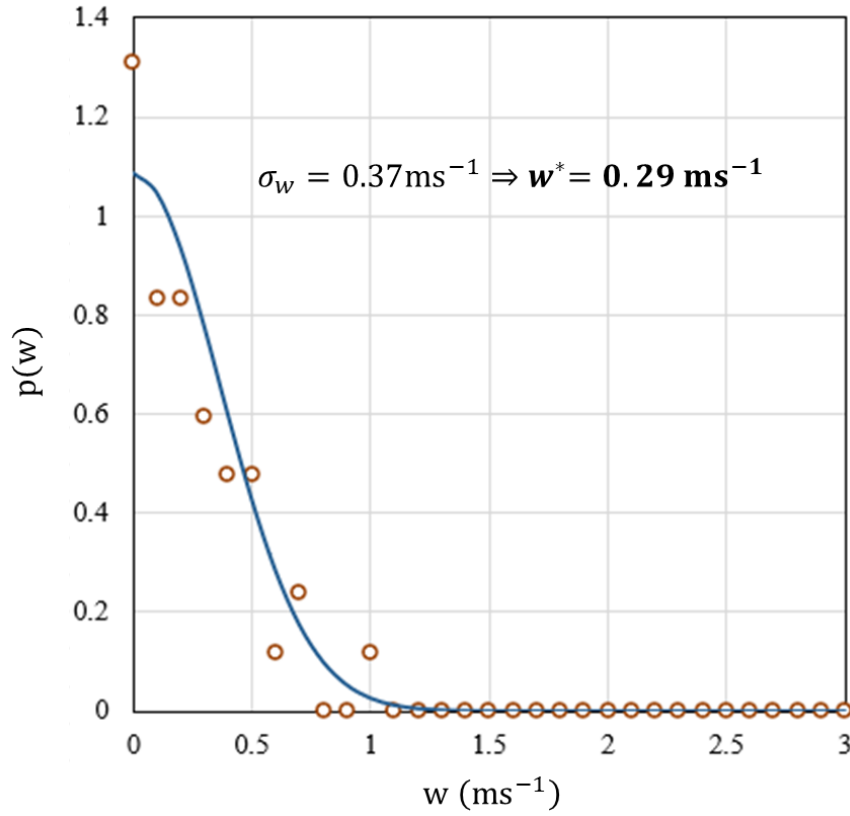


Figure S2. Example of the fitting of positive vertical velocities to a half-Gaussian probability density function, $p(w)$. The standard deviation of the distribution, σ_w , is then used within the droplet activation parameterization to calculate the characteristic vertical velocity, $w^*=0.79\sigma_w$ (Morales and Nenes, 2010), which is employed to provide the distribution-averaged cloud droplet number (N_d). The data presented here were collected at WOP and span the hourly time period between 17:00-18:00 UTC on 24 February 2019.

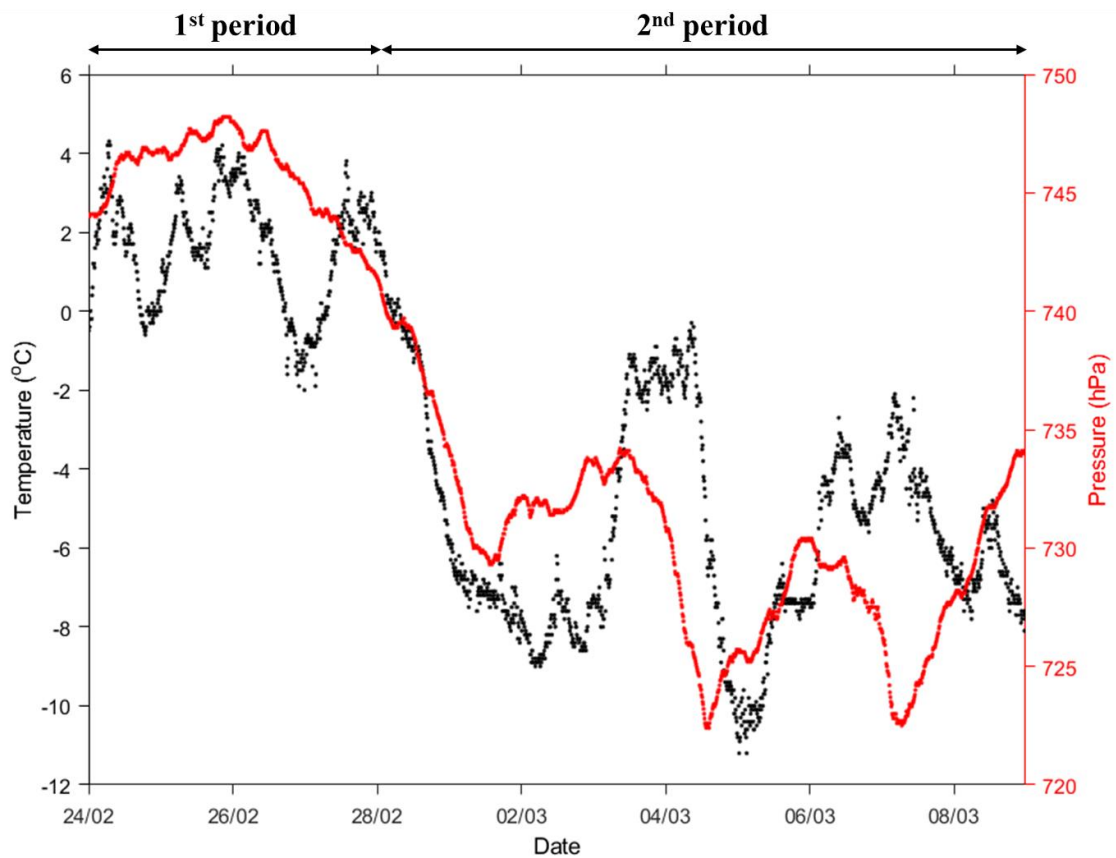


Figure S3. Air temperature 2 m above ground ($^{\circ}\text{C}$) (black dots) and pressure at station level (hPa) (red dots) obtained from the MeteoSwiss observation station at WFJ between 24 February and 8 March 2019.

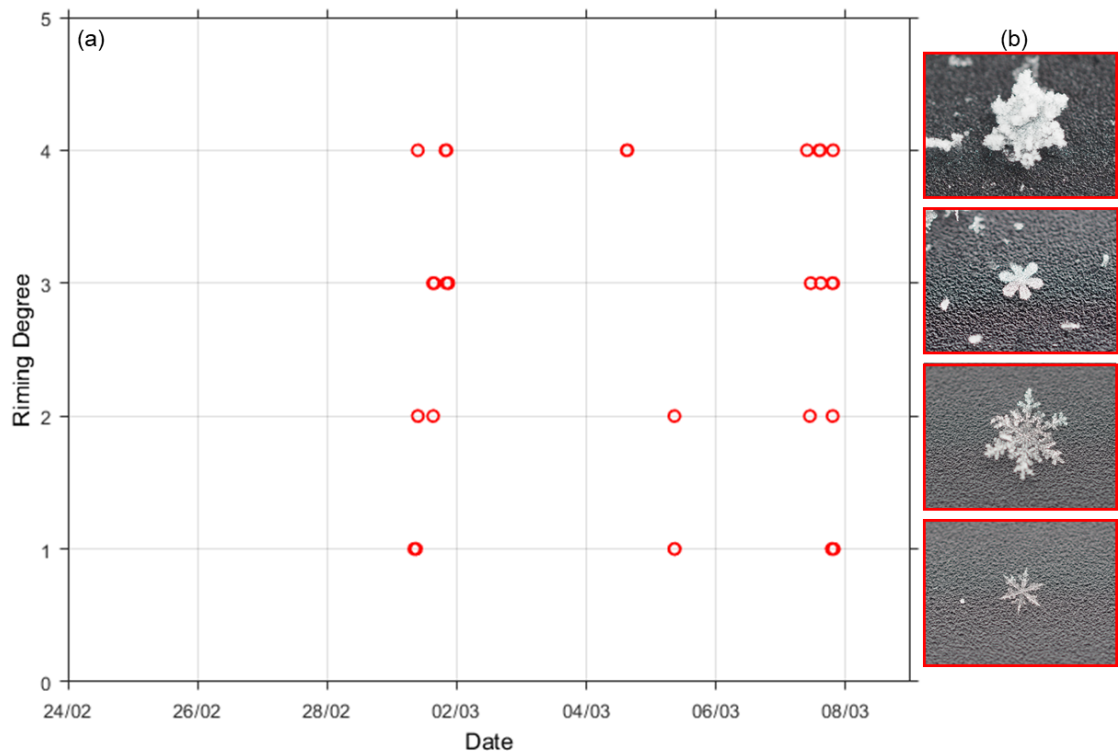


Figure S4. (a) The estimated degree of riming of the analyzed dendritic ice crystals collected at WFJ during the period of interest and (b) characteristic images of the dendrites representing the four recorded riming categories varying from 1 (bottom figure) to 4 (top figure). Following Mignani et al. (2019), dendritic crystals were collected on a plate and documented by photography. The resulting images were analyzed visually for a riming degree according to Mosimann et al. (1994). A riming degree of 1, 2, 3, 4 represents lightly, moderately, densely or heavily rimed ice particles, respectively.

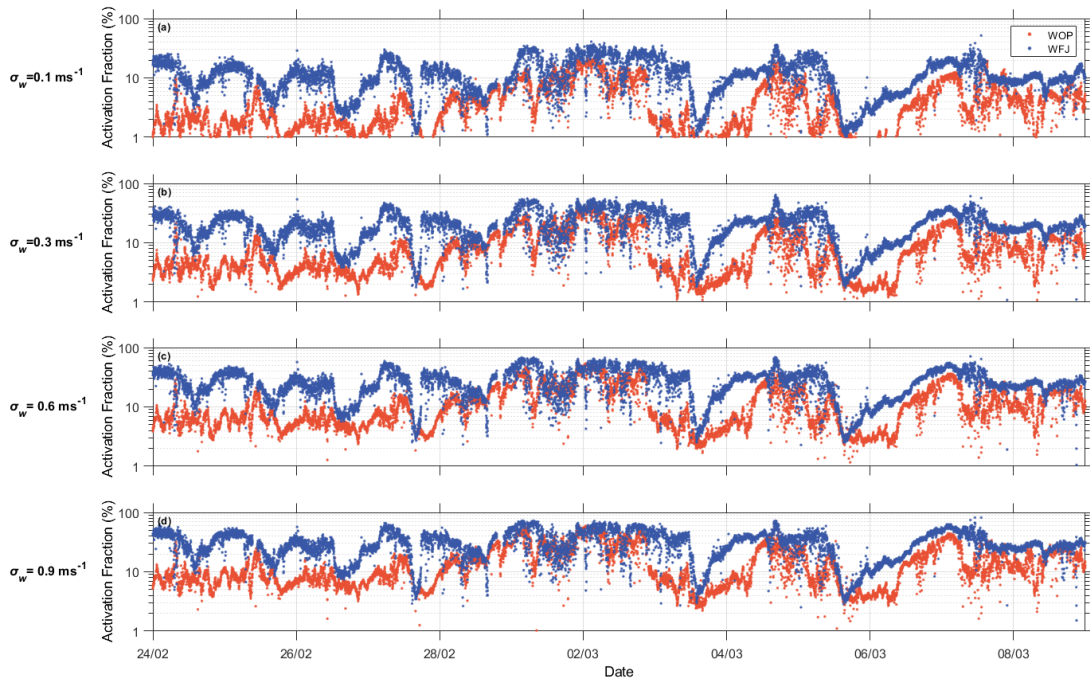


Figure S5. Calculated timeseries of the activation fraction (%) (i.e. the fraction of total aerosol particles that have been activated to form cloud droplets), for updraft velocities of $\sigma_w = 0.1 \text{ ms}^{-1}$ in a, 0.3 ms^{-1} in b, 0.6 ms^{-1} in c, and 0.9 ms^{-1} in d, during the period of interest at WOP (orange dots) and WFJ (blue dots).

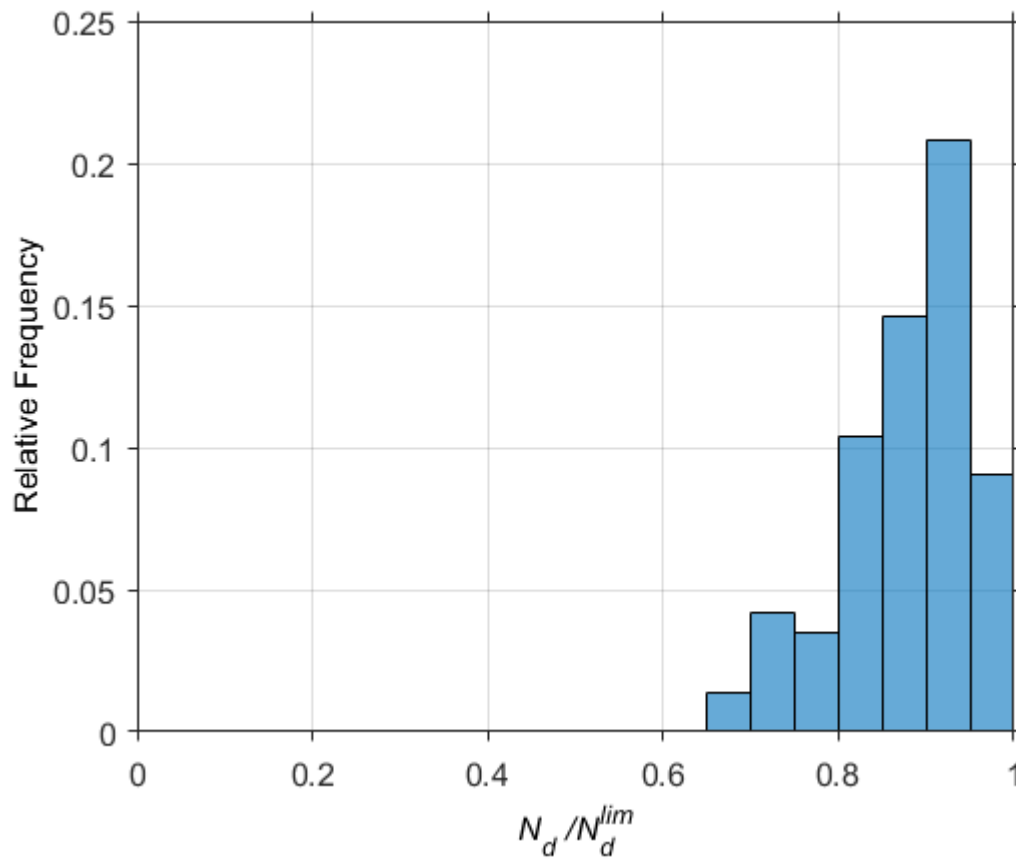


Figure S6. Relative frequency histogram of the ratio of predicted N_d to the limiting droplet number (N_d^{lim}), as calculated for both measurement sites, restricted to the periods when the predicted in-cloud maximum supersaturation (S_{max}) drops below 0.1%, indicating the transition from the aerosol- to the velocity-limited droplet activation regime.

References

- Mignani, C., Creamean, J. M., Zimmermann, L., Alewell, C., and Conen, F.: New type of evidence for secondary ice formation at around $-15\text{ }^{\circ}\text{C}$ in mixed-phase clouds, *Atmos. Chem. Phys.*, 19, 877–886, doi:10.5194/acp-19-877-2019, 2019.
- Morales Betancourt, R. and Nenes, A.: Characteristic updrafts for computing distribution-averaged cloud droplet number and stratocumulus cloud properties, *J. Geophys. Res.*, 115, D1822, doi:10.1029/2009JD013233, 2010.
- Mosimann, L, Weingartner, E. and Waldvogel A.: An analysis of accreted drop sizes and mass on rimed snow crystals., *J. Atmos. Sci.*, 51, 1548–1558, 1994.